



## **University of Huddersfield Repository**

Xu, X., Xu, H., Deng, H., Gu, Fengshou and Talbot, Chris J.

An investigation of a hypocycloid mechanism based twin-rotor piston engine

### **Original Citation**

Xu, X., Xu, H., Deng, H., Gu, Fengshou and Talbot, Chris J. (2014) An investigation of a hypocycloid mechanism based twin-rotor piston engine. *Proceedings of the Institution of Mechanical Engineers, Part C: Journal of Mechanical Engineering Science*. ISSN 0954-4062

This version is available at <http://eprints.hud.ac.uk/id/eprint/20137/>

The University Repository is a digital collection of the research output of the University, available on Open Access. Copyright and Moral Rights for the items on this site are retained by the individual author and/or other copyright owners. Users may access full items free of charge; copies of full text items generally can be reproduced, displayed or performed and given to third parties in any format or medium for personal research or study, educational or not-for-profit purposes without prior permission or charge, provided:

- The authors, title and full bibliographic details is credited in any copy;
- A hyperlink and/or URL is included for the original metadata page; and
- The content is not changed in any way.

For more information, including our policy and submission procedure, please contact the Repository Team at: [E.mailbox@hud.ac.uk](mailto:E.mailbox@hud.ac.uk).

<http://eprints.hud.ac.uk/>

# An investigation of a hypocycloid mechanism based twin-rotor piston engine

Xiaojun Xu<sup>\*1</sup>, Hao Deng<sup>1</sup>, Haijun Xu<sup>1</sup>, Fengshou Gu<sup>2,3\*</sup>, Chris Talbot<sup>3</sup>

<sup>1</sup>College of Mechatronics and Automation, National University of Defense Technology,  
Changsha, China

<sup>2</sup>Guest Researcher of Department of Vehicle Engineering at Taiyuan University of Technology Taiyuan, Shanxi, China

<sup>3</sup>Centre for Efficiency and Performance at the University of Huddersfield UK

\*Corresponding author

## Abstract

A unique mechanism is investigated in this paper to show the working principles of a novel hypocycloid twin-rotor piston engine (HTRPE), which provides the basis for the structural design, kinematic and dynamical analysis necessary to realize the engine. As a critical system in the HTRPE, the Differential Velocity Mechanism (DVM) is examined by decomposing it into two non-uniform motion mechanisms and a hypocycloid mechanism and performing an evaluation using different options of design parameters. Then analytical expressions for the rotor angular velocities and the relative angular velocities of pairs of rotors are derived for detailed performance analysis. Based on the results of this analysis a prototype HTRPE is suggested and benchmarked with both conventional reciprocating and Wankel engines. It is shown that the new engine outperforms the other two engines in key engine features including combustion gas force transmission, volumetric change of working chambers, power frequency, piston velocity and displacement, demonstrating that HTRPE is a very promising as a more energy efficient engine.

## Key words

Twin rotor, piston engine, Wankel engine, comparison, internal combustion engine.

## Introduction

Conventional reciprocating piston engines have been used widely for many years because of their high efficiency. However, they have a number of drawbacks such as complicated and costly valve systems, a high level of vibration due to unbalanced piston masses, and relatively small power to mass ratio<sup>[1]</sup>. For more than one century, numerous types of novel engine mechanisms have been proposed and patented<sup>[2, 3]</sup>. For example, the SYTech engine based on the scotch yoke mechanism was developed by CMC Power Systems in Sydney<sup>[4]</sup>. The Cardan gear mechanism was compared with the conventional slider-crank mechanism in air pumps and four-stroke engines<sup>[5]</sup>. These types of novel engines have been proposed as means of reducing the inherent disadvantages of reciprocating engines<sup>[6-9]</sup>.

However, the most promising option is the “rotary engine” as the reciprocating engine has been developed to a near-perfect state with further improvement becoming ever more difficult and costly to achieve. The Wankel engine<sup>[10]</sup> has the most potential in terms its simple construction and rotor based working processes, consequently it has attracted a lot of development efforts and funds. However in practice it has been found that it also is subject to many problems including sealing difficulties, poor combustion conditions, high manufacturing challenges and low maintainability. Therefore, with the growing requirement of high efficiency and low emissions in recent years more and more researchers have paid attention to reconsidering or designing alternative types of rotary engines<sup>[11, 12]</sup>.

Amongst different variants, oscillatory rotation type engines have gained a prominent development<sup>[13-15]</sup> for their high compactness and simple construction. However, it is shown in the published literature<sup>[16-18]</sup> that many proposals based on ratchet stops, cams, elliptical gears, half rounded and other special gears for this type of engine seem unreliable, or have difficulty withstanding the excessive shocks which are inherent in internal combustion engines.

To overcome the deficiency of existing developments the authors in [19] presented a basic structure and working principles of a novel oscillatory rotating engine called the Twin-Rotor Piston Engine (TRPE). The TRPE is based on a number of newly invented mechanisms<sup>[20, 21]</sup>, allowing the realization of a high power density. Fig. 1 illustrates the key features of the first prototype TRPE. As shown it consists of two mechanical systems. One is the energy conversion system (ECS) and the other is a differential velocity mechanism (DVM). The ECS is designed to convert heat energy into mechanical energy, and the DVM is for converting two non-uniform rotations into a uniform one. In developing the prototype, the TRPE has been confirmed to be effective in terms of sealing, construction and power density.

As shown in Fig.1(b) a typical DVM for the first prototype TRPE consists of a stationary gear ring, two planetary gears, two connecting rods and two rockers. The planet carrier (*AO*), the crank (*AB*), the connecting rod (*BC*) and the front rocker (*OC*) constitute a crank-rocker mechanism. In the same way, the other components connected to the rear rocker constitute a second crank-rocker mechanism denoted

by dashed symbols. As the front rocker is fixed to one rotor and the rear rocker to an adjacent rotor, the rotation of the two rotors follows a cyclical oscillatory motion due to their respective crank-rocker mechanisms. The volume of a chamber formed by a vane piston fixed on one rotor and an adjacent piston on the other rotor will vary with the angular positions of the rotors so that they will realize the full working cycle as in a conventional internal combustion engine. As shown in Figure 1 (a) there are six vane pistons uniformly mounted on each rotor. This means that there can be six working cycles per one revolution of the output shaft, showing that the mechanisms allow multiple combustions per revolution and consequently produce more power in a limited space. In addition, because of surface contact between the piston and enclosure, it will be much easier for sealing compared to the line contact of the Wankel engine.

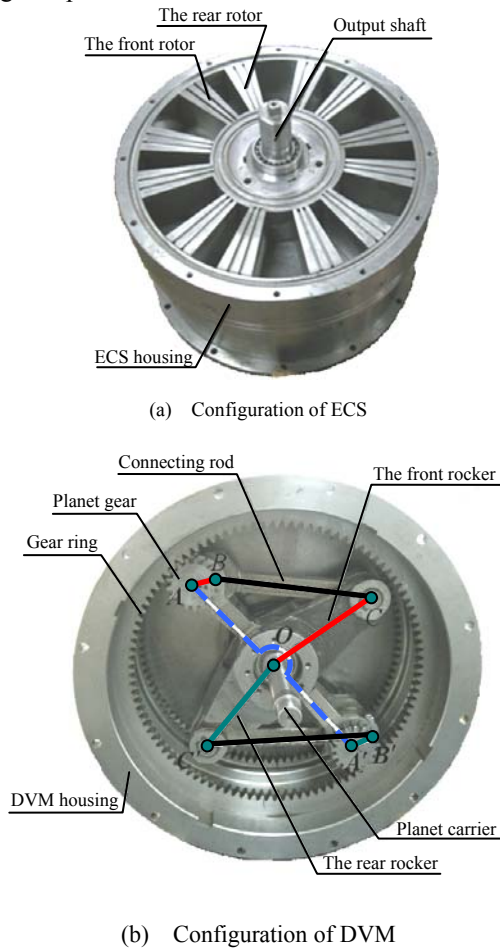


Fig. 1. Illustrative photos of the first prototype TRPE

For an in-depth understanding of the TRPE, necessary for examining its kinematics and dynamics and for the optimization of components in designing it, its DVM system is further investigated in this study by decomposing it into two non-uniform motion mechanisms and a hypocycloid mechanism. In the meantime other variants of the DVM are also investigated for optimal parameter selection. With this understanding the analytic expression of the rotor velocity and their relative velocity for a new prototype is also derived, which allows a more accurate

comparison with two conventional engines to demonstrate the key features of the new TRPE.

## The differential velocity mechanism (DVM) of the HTRPE

A DVM used in the first prototype TRPE has been studied in [19, 22]. To improve the performance of the suggested TRPE, this section introduces a similar type of DVM but based on a different mechanism whose kinematics are examined by decomposing the mechanism into two non-uniform motion mechanisms and a hypocycloid mechanism.

### Parameter design of DVM

#### The non-uniform motion mechanism.

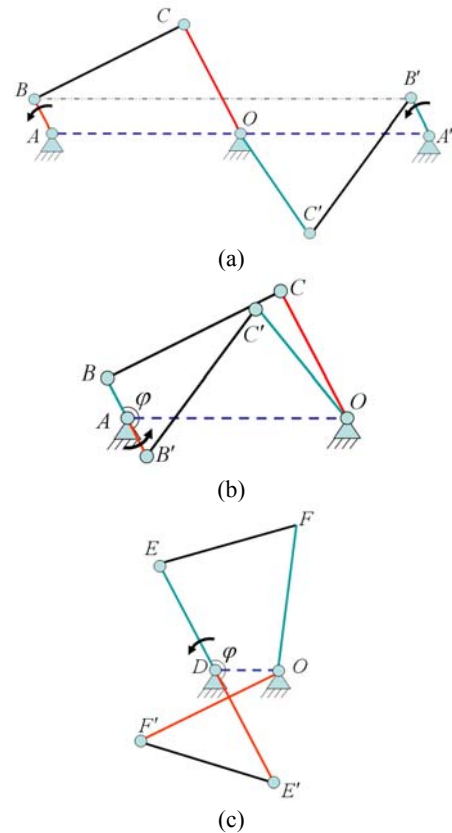


Fig. 2. Three variants of the non-uniform motion mechanisms with  $180^\circ$  phase differences : (a) The two crank-rocker mechanisms with parallel crank; (b) The two crank-rocker mechanisms with crank collinear; and (c) The two double-crank mechanisms with crank collinear.

For ease of understanding Fig. 1 (b) is schematically reproduced in Fig. 2(a). In the meantime two other variants of the mechanism with different design parameters, which can also be considered for TRPE, are presented in Fig. 2(b) and 2(c) for performance and construction comparison. These three non-uniform motion mechanisms have the same length parameters, but their driven parts are denoted by  $AB$  and  $A'B'$ ,  $AB$  and  $AB'$ ,  $DE$  and  $DE'$  respectively with a phase difference of  $\varphi$  (shown as  $180^\circ$ ).

As the driving parts denoted by  $OC$  and  $OC'$ ,  $OF$  and  $OF'$  respectively rotate at a constant speed, the relative motion of the corresponding driven parts of  $AB$  and  $A'B'$ ,  $AB$  and  $AB'$ ,  $DE$  and  $DE'$  produce non-uniform motions, which are just the oscillatory rotations desired for the TRPE. As shown in Fig. 1 (b), two rotors can be fixed directly to the two driven parts such as  $AB$  and  $A'B'$  in the mechanism in Fig. 2 (a). Thus, the rotors can rotate at a variable speed, allowing two reference positions on each rotor to move towards and away from each other, realizing the engine working cycle.

Obviously, it is much easier to realize the mechanism of Fig. 2 (a) in a TRPE and the following discussion will be based on this configuration.

**The hypocycloid mechanism.** However, the engine cycle can be obtained only once per revolution of the output shaft when the mechanism in Fig. 2 is applied straightforwardly. Obviously, this direct application based on the TRPE cannot increase the power density.

To increase the power density this paper proposes to repeat the oscillatory motion of the driven parts so that they can achieve multiple engine cycles in one revolution of the output shaft. To realize this, a hypocycloid mechanism is employed because a hypocycloid produces a cyclical and symmetrical curve which is fully defined mathematically and can also be realized easily by existing manufacturing systems. The simplest type of the hypocycloid mechanism consists of a stationary gear ring, a planet gear and a planet carrier, in which a gear ratio is defined as

$$i = \frac{r_1}{r_2} \quad (1)$$

where  $r_1$  is the radius of the gear ring and  $r_2$  is the radius of the planet gear. As shown in Fig. 3(a), when the planet gear rotates inside the stationary gear ring, the joint  $B$  on the planet gear will follow a hypocycloidal trajectory. Supposing that the gear carrier ( $OA$ ) rotates in the counter-clockwise (c.c.w.) direction, then the planet gear ( $AB$ ) will rotate in a clockwise direction with an angle of  $i\theta_1$  if the gear carrier rotates through an angle of  $\theta_1$ . If  $l_{AB}$  is the distance from the center of the joint  $B$  to the center of the planet gear, a dimensionless parameter  $\rho$  is defined as the ratio between the distances  $l_{AB}$  and the planet gear radius  $r_2$ :

$$\rho = \frac{l_{AB}}{r_2} \quad (2)$$

For  $\rho < 1$ ,  $= 1$ , and  $> 1$ , the joint will be located inside, on the pitch circle and outside of the planet gear respectively. Following the resulting motion the coordinates  $B_x$  and  $B_y$  of the joint  $B$  on the planet gear follow a hypocycloidal curve which is expressed by

$$\begin{cases} B_x = r_2[(i-1)\cos(\theta_1) + \rho \cos((1-i)\theta_1)] \\ B_y = r_2[(i-1)\sin(\theta_1) + \rho \sin((1-i)\theta_1)] \end{cases} \quad (3)$$

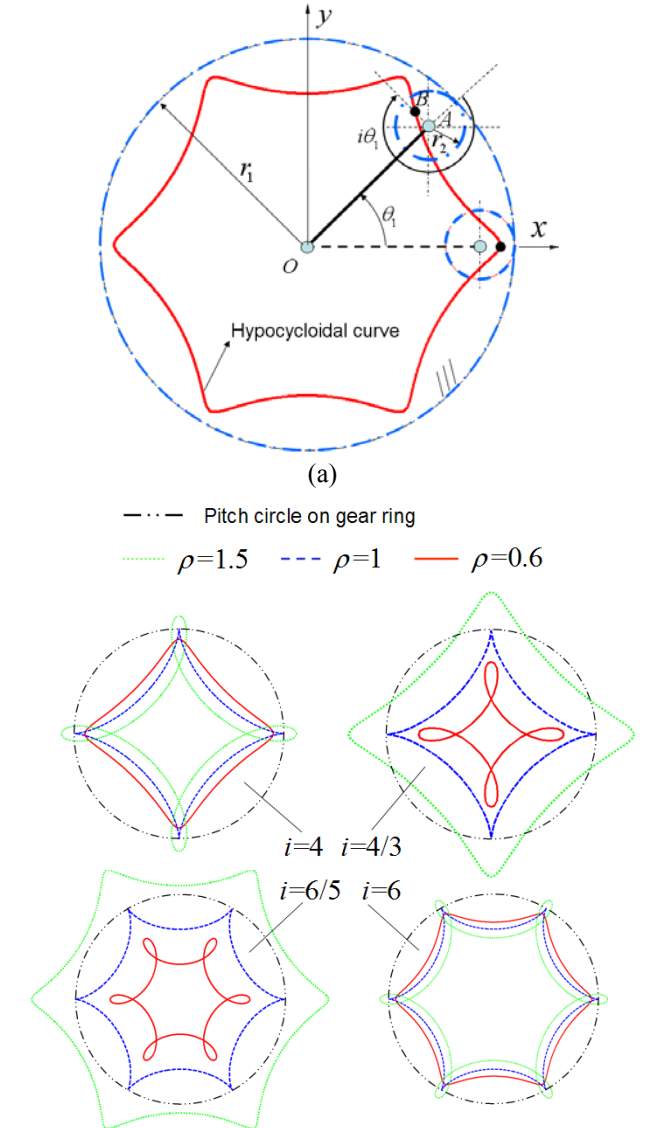


Fig. 3. Mathematical model of hypocycloid curves with different parameters: (a) Mathematical model of hypocycloid; (b) hypocycloid curves with different parameters

As shown in Fig. 3(b), it can be seen that the shape of the hypocycloidal curve is essentially determined by the parameters  $i$  and  $\rho$ . Considering an integer number of gear teeth, the gear ratio  $i$  in (1) will be represented as

$$i = \frac{N}{M} \quad (4)$$

where  $N > M$  and both  $N$  and  $M$  are integers and are relatively prime numbers. As shown in Fig. 3(b), there are many possible hypocycloid curves.  $N$  is equal to the number of cusps on the hypocycloid curves.  $M$  is equal to the number of revolutions of the planet carrier which is needed to form a periodic hypocycloid curve.

However, in order to generate hypocycloid curves that can be used as the trajectory of HTRPE mechanisms,  $M$  has to meet the condition of

$$M = 1 \text{ or } M = N - 1 \quad (5)$$

In addition, to make sure that the hypocycloid curves generated by  $M = 1$  and  $M = N - 1$  are the same, the conditions in (6) should be met:

$$\begin{cases} l_{AB} = l_{OD} = r_3 - r_4 \\ l_{OA} = l_{DE} = r_1 - r_2 \\ l_{OC} = l_{OF}, l_{BC} = l_{EF} \\ \frac{r_2 + r_4}{r_1 - r_3} = 1 \end{cases} \quad (6)$$

Based on these conditions, there are at least three possible arrangements for the DVM by using different configurations of the non-uniform motion mechanism and values of  $M$ , which are illustrated in Fig. 4. However, the arrangement (a) in Fig. 4 will be further investigated in following sections for its advantages of easy construction.

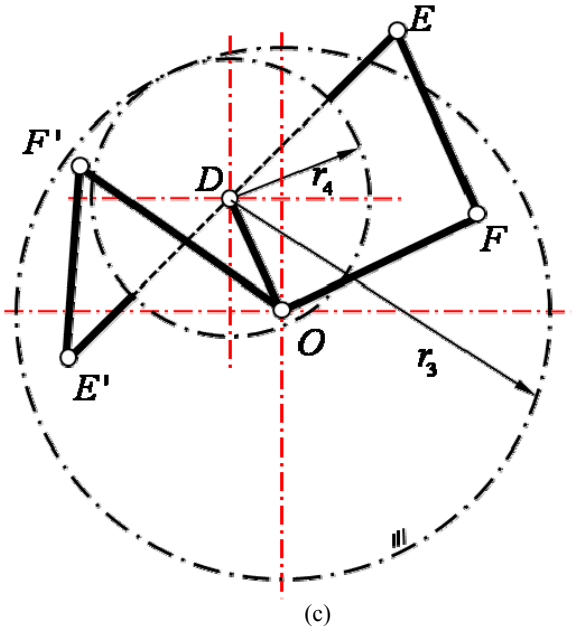
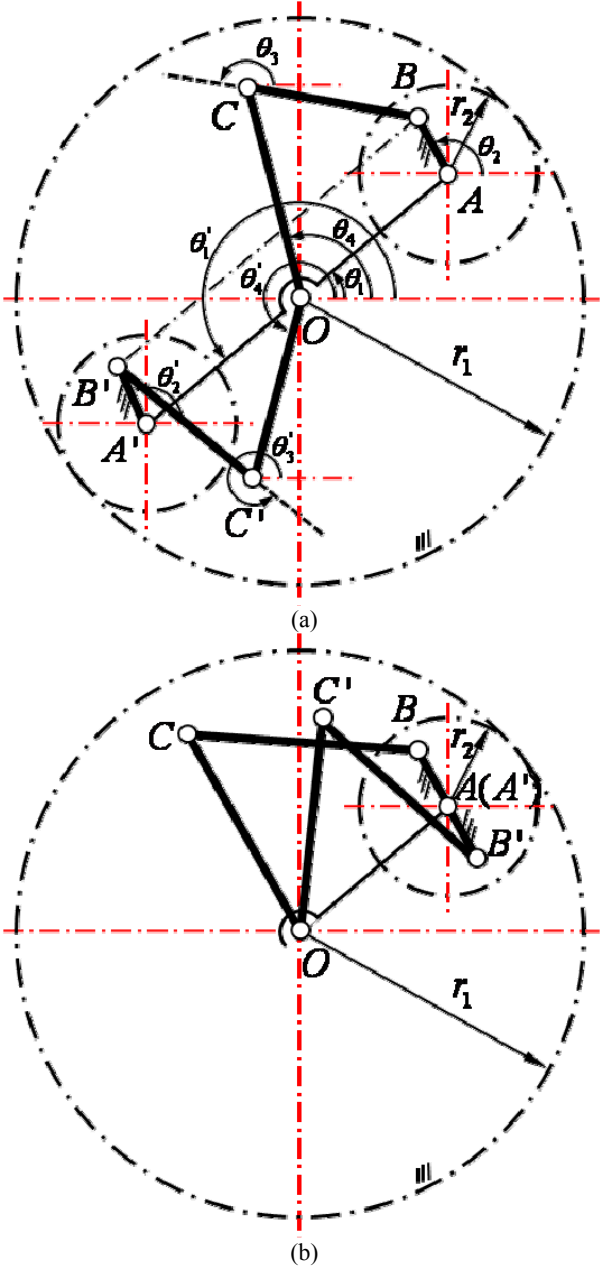


Fig. 4. Three options for DVM: (a) DVM with parallel crank with  $i=N$ ; (b) DVM with crank collinear with  $i=N$ ; (c) DVM crank collinear with  $i=N / (N-1)$ . Where  $OA = OA' = l_1$ ,  $AB = A'B' = l_2$ ,  $BC = B'C' = l_3$ ,  $OC = OC' = l_1$ .

#### Kinematics of the DVM

To see the motion characteristics of the DVM shown in Fig. 4 (a), its kinetic equations can be developed using a loop closure method [19] as follows

$$\begin{cases} l_1 \cos \theta_1 + l_2 \cos \theta_2 + l_3 \cos \theta_3 = l_4 \cos \theta_4 \\ l_1 \sin \theta_1 + l_2 \sin \theta_2 + l_3 \sin \theta_3 = l_4 \sin \theta_4 \\ l_1 \cos \theta'_1 + l_2 \cos \theta'_2 + l_3 \cos \theta'_3 = l_4 \cos \theta'_4 \\ l_1 \sin \theta'_1 + l_2 \sin \theta'_2 + l_3 \sin \theta'_3 = l_4 \sin \theta'_4 \end{cases} \quad (7)$$

where the definitions of  $l_1 \sim l_4$ ,  $\theta_1 \sim \theta_4$ , and  $\theta'_1 \sim \theta'_4$  are following [19], and  $\theta_1 = \theta'_1$ ,  $\theta'_2 = \theta_2 = (1-i)\theta_1$ . So  $\theta_3$ ,  $\theta'_3$ ,  $\theta_4$ ,  $\theta'_4$  can be obtained when  $\theta_1(t)$  is assumed to be known. For the case  $\theta_1(t) = \omega_0 t$  ( $\omega_0$  is the angular velocity of the output shaft of the TRPE), the angular displacement of  $\theta_4$ , for example, can be deduced as

$$\theta_4 = 2 \arctan \left( \frac{L \pm \sqrt{K^2 + L^2 - M^2}}{M + K} \right) \quad (8)$$

where,

$$K = l_1 \cos \theta_1 + l_2 \cos \theta_2$$

$$L = l_1 \sin \theta_1 + l_2 \sin \theta_2$$

$$M = (K^2 + L^2 + l_4^2 - l_3^2) / (2l_4)$$

$$N = (l_4^2 - l_3^2 - K^2 - L^2) / (2l_3)$$

Moreover,  $\omega_4$  can be also obtained by differentiating (8) with respect to time to give :

$$\omega_4 = \omega_1 - i\omega_1 \frac{l_1 l_2 \sin(i\theta_1) - l_2 l_4 \sin[\theta_4 - (1-i)\theta_1]}{l_1 l_4 \sin(\theta_1 - \theta_4) - l_2 l_4 \sin[\theta_4 - (1-i)\theta_1]} \quad (9)$$

$\theta'_4$  and  $\omega'_4$  can be also derived in the same way to give

$$\omega'_4 = \omega_1 - i\omega_1 \frac{l_1 l_2 \sin(i\theta_1) + l_2 l_4 \sin(\theta'_4 - (1-i)\theta_1)}{-l_1 l_4 \sin(\theta'_4 - \theta_1) + l_2 l_4 \sin(\theta'_4 - (1-i)\theta_1)} \quad (10)$$

In the isolated crank-rocker mechanism *OABC* in Fig. 4, the ratio between the angular velocity of the crank *AB* and the angular velocity of the rocker *OC* is

$$\frac{\omega_{OC}}{\omega_{AB}} = \frac{l_2 l_1 \sin \theta_{21} + l_2 l_4 \sin(\theta_{42})}{l_4 l_1 \sin \theta_{41} + l_2 l_4 \sin(\theta_{42})} \quad (11)$$

where  $\theta_{21} = \theta_2 - \theta_1$  is defined as the relative angle between the crank and the frame, and  $\theta_{42} = \theta_4 - \theta_2$  is defined as the relative angle between the rocker and the frame. Thus Eq. (9) has the following form:

$$\omega_4 = \omega_1 + \omega_{21} \frac{\omega_{OC}}{\omega_{AB}} \quad (12)$$

where  $\omega_{21} = -i\omega_1$  represents the angular velocity of the planet gear with respect to the planet carrier. Eq. (12) shows that the angular velocity of the rotor is the combination of two motions. Moreover, it also demonstrates that it is feasible to decompose the DVM into two non-uniform motion mechanisms and a hypocycloid mechanism to gain a good understanding of it.

To study the speed characteristics between two rotors,  $\omega_r$  is defined as the relative angular velocity between them and can be expressed as

$$\omega_r = \omega_4 - \omega'_4 \quad (13)$$

Theoretically, it is hard to find a simple expression for  $\omega_r$ . However, a numerical simulation can be carried out to find its variation with respect to the rotation angle of the output shaft. Based on the assumptions of section 2.2, an analytic expression for  $\omega_r$  can be derived as

$$\omega_{rt} = \frac{N\omega(\delta_{max} - \delta_{min})}{2} \sin N\theta \quad (14)$$

where  $\theta$  and  $\omega$  are the angular position and velocity of the output shaft respectively. In general, the output shaft is fixed on the planet carrier. So  $\theta = \theta_1$  and  $\omega = \omega_1$ . Fig. 5 shows the comparison between  $\omega_r$  and  $\omega_{rt}$  for parameters values:  $N = 6$ ,  $r_1 = 150mm$ ,  $l_2 = 12mm$ ,  $l_3 = 205mm$ ,  $l_4 = 144mm$ ,  $\omega_1 = 1(r/min)$  which are the same as in [19]. It can be seen from Fig.5 that  $\omega_{rt}$  is nearly the same as  $\omega_r$  other than a phase delay due to the difference in the initial conditions. Moreover, the result also shows that the volume of the working chamber of the HTRPE varies approximately sinusoidally with respect to angular position.

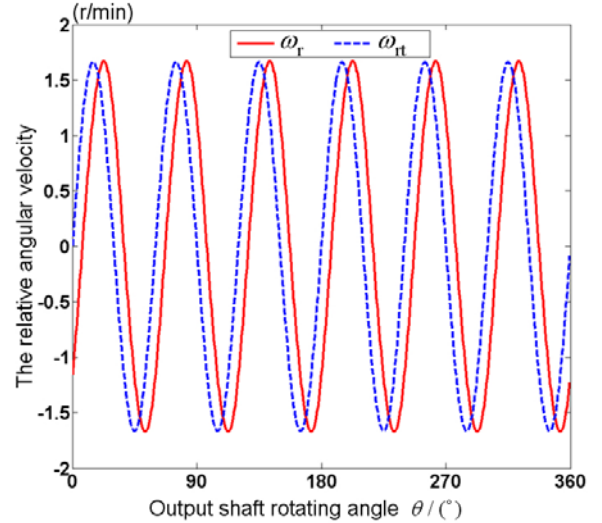


Fig. 5. Comparison between the numerical value of the relative angular velocity derived from the suggested expression and that of analytic expression

## Comparison of performance between three piston Engines

With the kinetics developed, the performance of the HTRPE can be examined, allowing a comparison to be made with that of two other types of conventional engines: the reciprocating engine and the Wankel engine.

### Combustion gas forces

As shown in Fig. 6, to produce torque all piston engines rely on the expansion pressure  $p_{ig}$  produced by the combusting gas mixture. The difference between the mechanisms of these three different engines is in the expansion pressure that is used. In the reciprocating (or Wankel) engine,  $p_{ig}$  is generated as the combustion chamber forces the piston down (or turns the rotor). The mechanical force  $F$  from  $p_{ig}$  can be decomposed into two components: the force toward the centre of the output shaft denoted by  $F_n$  and the tangential force denoted by  $F_t$ . Only  $F_t$  rotates the output shaft.

For the HTRPE, the direction of the gas pressure acting on the rotors is always perpendicular to the surface of the vane pistons. As shown in Fig.6(c) the effects of driving the front rotors by the three gas forces:  $\mathbf{F}_1$ ,  $\mathbf{F}_2$ , and  $\mathbf{F}_3$  (or  $\mathbf{R}_1$ ,  $\mathbf{R}_2$ , and  $\mathbf{R}_3$ ) are the same. It can be seen that the vector sum of combustion gas forces acting on each rotor is a pure torque. In addition, there exists no radial force between the two rotors and the housing and no radial forces on the bearing.

Another feature is that there is a large contact area between the vane piston skirt and the inner surface of the housing, so the sealing problems of the HTRPE are much easier to solve than those of other rotary engines such as the Wankel (having a line contact between the rotor and

housing is a serious obstruction to extending its application).

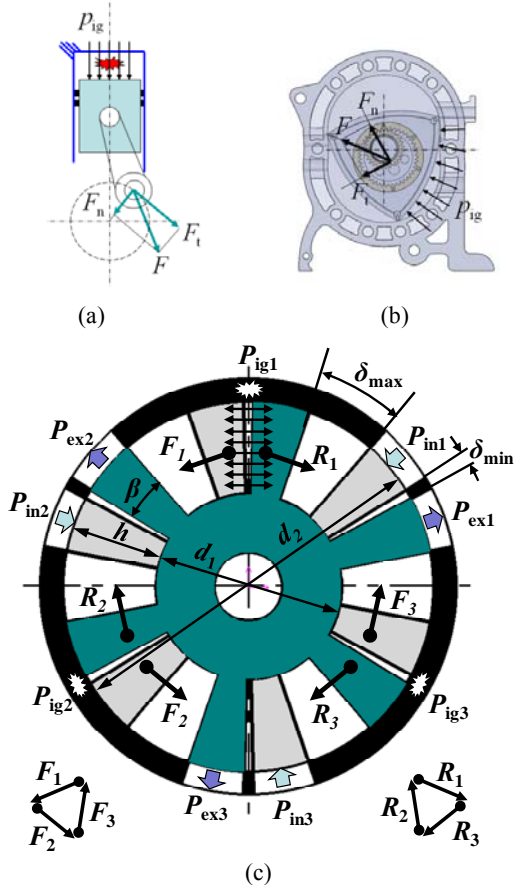


Fig. 6. The pistons under combustion gas pressure in the (a) reciprocating engine, (b) Wankel engine, and (c) HTRPE with  $N=3$

#### Volumetric change of working chamber

Table 1 and Fig. 7 show the characteristics of the working chamber for the three engines. Firstly, the shape change of working chambers in the HTRPE is similar to that of the reciprocating engine. Both of them have a linear variation. The change of former is along the length  $x$  of working chamber from  $t_1$  to  $t_2$  while the latter is relative to the fan angle of the working chamber  $\delta$ . Secondly, the number of working chambers per cylinder  $Z$  and the overall shape of working chamber are different among the three engines. In general, with the fan shaped working chambers and the linear variation of chamber shape, the HTRPE has the same advantage as the reciprocating engine in flame spread and uniform combustion.

**Table 1. Characteristics of working chambers for (a) reciprocating engine, (b) Wankel engine, and (c) HTRPE**

Engine	$\Delta V$	$Z$	Shape
(a)	$S[x(t_2) - x(t_1)]$	1	Rectangle
(b)	~	3	Crescent
(c)	$k_v[\delta(t_2) - \delta(t_1)]$	$N$	Fan

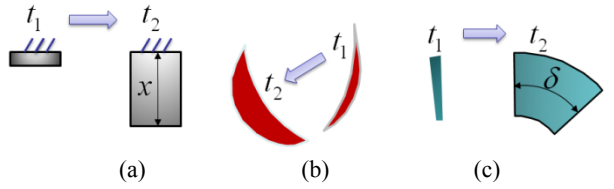


Fig. 7. Comparison of shape change of working chambers in the (a) reciprocating engine, (b) Wankel engine, and (c) HTRPE

**Volume of the working chamber in the reciprocating engine.** For a more detailed comparison, the volumetric characteristics are calculated over a full operating cycle. For the reciprocating engine

$$V = V_{\min} + Sx \quad (15)$$

where  $x = R(1 - \cos \theta + \frac{\lambda}{2} \sin^2 \theta)$ ,  $S$  is the area of cylinder,  $R$  is radius of the crank,  $\lambda$  is defined as  $L/R$ ,  $L$  is the length of the connecting rod.

For Wankel engine the volume of the working chamber is expressed as<sup>[10]</sup>

$$V = V_{\min} + \frac{3\sqrt{3}}{3} eR_w b [1 - \sin(\frac{2}{3}\theta + \frac{\pi}{2})] \quad (16)$$

where the value of  $V_{\min}$  is calculated according to Ref. [10],  $b$  is the width of the rotor housing,  $R_w$  is the generating radius,  $e$  is the eccentricity,  $\varphi_{\max}$  is the maximum angle of oscillation, and  $\varphi_{\max} = \arcsin(3e/R)$ .

According to section 3 the volume of the working chamber of the HTRPE can be expressed as<sup>[19]</sup>

$$V = k_v \delta \quad (17)$$

where  $\delta$  follows a sinusoidal process:

$$\delta = -\frac{\delta_{\max} - \delta_{\min}}{2} \cos N\theta + \frac{\delta_{\max} + \delta_{\min}}{2} \quad (18)$$

And  $k_v = [(d_2)^2 - (d_1)^2]h/8$ .

For a direct comparison,  $V_{\min}$  of the three engines is assumed to be the same, so  $\delta_{\min} = V_{\min}/k_v$ . Fig. 8 shows the plot of volumetric change against shaft angle for the three engines. It can be seen that the volumetric change in the HTRPE is similar to that of the two conventional engines. Furthermore, the period of the volumetric change in the HTRPE is 1/4 of that of the reciprocating engine and 1/6 of that of the Wankel engine, showing that the HTRPE has a significantly higher power frequency.

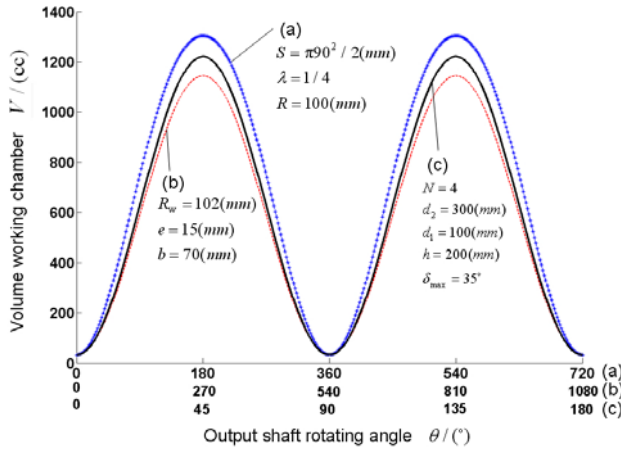


Fig. 8. Comparison of change in volume of working chamber in the (a) reciprocating engine, (b) Wankel engine, and (c) HTRPE

### Power frequency

The basic concept of the HTRPE is very similar to that of the Wankel engine. The Wankel engine performs the four-stroke cycle without using any valve mechanism and has one power stroke per revolution of the output shaft, as in the case of a two-stroke reciprocating engine. Both Wankel engines and two-stroke reciprocating engines have superb features of light weight and compactness. So engines with more power strokes per revolution may be able to generate a higher power to weight ratio than conventional engines. In this way, the HTRPE is like the Wankel engine and also exhibits these characteristics.

Table 2 shows a comparison of conventional L4 engine, Wankel engine and HTRPE with 4, 6, 8 vane pistons which are named HTRPE-4, HTRPE-6, and HTRPE-8 respectively.  $C$  is defined as the number of power strokes per revolution of the output shaft<sup>[19]</sup>, and  $C=N^2$ .  $X$  is defined as the number of working chambers in combustion at any time.

Table 2. Comparison of power frequency of conventional L4 engine, Wankel engine and HTRPEs

Engine Type	$Z$	$C$	$X$
L4	4	2	1
Wankel	3	1	1
HTRPE-2	4	4	1
HTRPE-4	8	16	2
HTRPE-6	12	36	3

Taking L4 and HTRPE-4 as an example, it can be seen that both of them have the same four working chambers. However, HTRPE-4 has 16 power strokes per revolution of the output shaft whereas L4 has only 2 power strokes. Moreover, in HTRPE-4, the respective components of the four cycles are carried out simultaneously in diametrically opposed chambers. That is, the operations on one side of the engine are duplicated on the other side of the engine. This design ensures balanced pressure forces within the eight working chambers of the engine. Overall, HTRPE has the potential of higher power density due to

multiple utilization of work space during one revolution and higher uniformity of torque due to multiple work strokes within one revolution.

### Velocity of piston

Piston velocity is an important factor in determining the durability of the seal and the inner surface of the housing. The calculations of piston speed for three engines are summarized in Table 3, in which  $v_{\text{rec}}$  is the piston velocity in the reciprocating engine,  $v_{\text{wankel}}$  is the sliding speed of the rotor vertex over the inner surface of the housing in the Wankel engine and  $v_T$  is the circumferential velocity of the rotor in the HTRPE. Fig. 9 shows a numerical comparison of the speed between these three engines. It can be seen that in the case of reciprocating engine, the piston in reciprocating motion reverses in its sliding direction each time it reaches its top and bottom dead center. In the Wankel engine and the HTRPE, their rotors always rotate in the same direction eliminating the speed-zero point, which is clearly advantageous to the formation of a hydrodynamic oil film.

Table 3. Piston speed calculations of the three engines

Engine	Piston speed
(a)	$v_{\text{rec}} = R\omega_0 \sin \theta + R\omega_0 \frac{\lambda}{2} \sin 2\theta$
(b)	$v_{\text{wankel}} = \frac{\omega_0}{3} \sqrt{(9e^2 + R_w^2 + 6eR_w \cos \frac{2}{3}\theta)}$
(c)	$v_T = \frac{d_2}{2} [\omega_0 + \frac{N\omega_0(\delta_{\max} - \delta_{\min})}{4} \sin N\theta]$

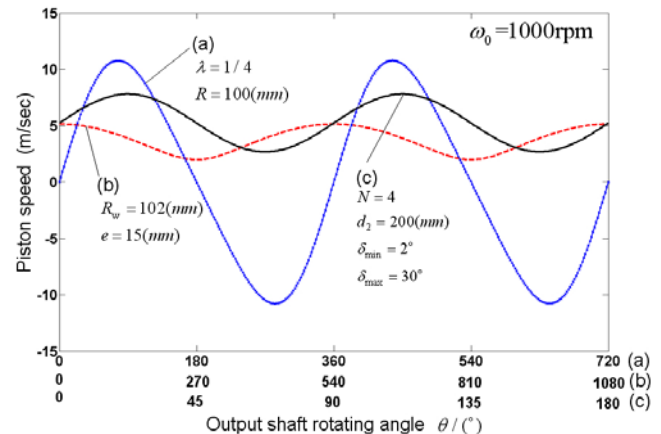


Fig. 9. Comparison of piston speeds for (a) reciprocating engine, (b) Wankel engine, and (c) HTRPE engine

### Displacement

The HTRPE has unique characteristics inherited from the features of its construction such as no reciprocating parts, the rotation of the working chamber with the rotor, etc. However, similar to Wankel engines, the HTRPE can also be evaluated with respect to performance characteristics as a displacement type internal combustion four-stroke engine.

The total displacement of the HTRPE can be calculated as [19]

$$Q_{ex} = \frac{N(\pi - N\beta)(d_2^2 - d_1^2)h(\varepsilon - 1)}{4(\varepsilon + 1)} \quad (19)$$

From Eq. (19), it can be seen that  $Q_{ex}$  is determined by the structure parameters of the HTRPE as well as the compression ratio  $\varepsilon$ . The HTRPE can be designed to be an engine with various choices of compression ratio, so it is necessary to calculate the effect on the displacement of the engine with. As shown in Fig. 10, it can be seen that  $Q_{ex}$  increases with increasing  $\varepsilon$  when the structure parameters are set to be  $N = 6$ ;  $\beta = 12^\circ$ ;  $d_2 = 300\text{mm}$  and  $h = 100\text{mm}$ . In particular at  $\varepsilon = 16$ ,  $Q_{ex} = 20\text{L}$ .

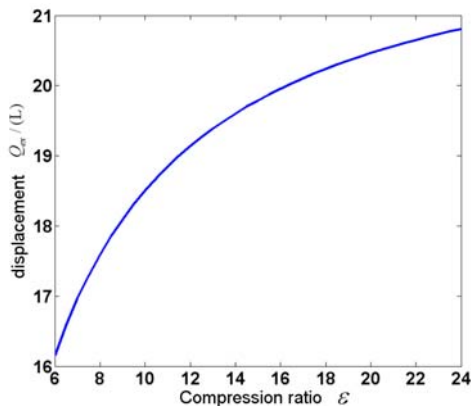


Fig.10. Displacement of the engine with respect to the compression ratio

The total gas volume  $I$  obtained during the intake or exhaust process in the HTRPE will be

$$I = \omega_0 Q_{ex} \quad (20)$$

Assume that the input energy of the HTRPE ( $E$ ) is proportional to  $I$ . So

$$E = k_e I \quad (21)$$

where  $k_e$  is a constant.

For a comparison made from the same base line, values of  $I$  for the three engines are chosen to be close each other for the same values of  $E$ .  $N_c$  is the number of cylinders of the engine,  $N_w$  is the number of working chambers of the engine and  $N_w = ZN_c$ ;  $\tau$  is defined as the power to weight ratio of the engine with  $\tau = P/M$ . Table 4 shows a comparison of a conventional L4 engine, a Wankel engine and the HTRPE. As the values of  $I$  for all engines are close to each other, these three engines have the same approximate input energy. On the other hand, the HTRPE has the promise of a greater power to weight ratio and a lower output shaft velocity.

Table 4. Comparison of a conventional L4 engine, a Wankel engine and the HTRPE

	HTRPE	Diesel engine	Mazda engine
$N = 6$	CA6DL1-32E3	787B-R26B	
$I(\text{L})$	20000	17710	23544
$N_c$	1	6	4

$N_w$	12	6	12
$Q_{ex}(\text{L})$	20	7.7	2.6
$\omega_0(\text{r/min})$	1000	2300	9000
$P(\text{kw})$	500	239	514
$M(\text{kg})$	100	780	180
$\tau(\text{kw/kg})$	5	0.306	2.85

## Conclusions

Compared with the two conventional engines, the HTRPE has potential advantages as follows:

- (1) The volume of the working chambers of the HTRPE varies sinusoidally with the output shaft rotation angle.
- (2) The vector sum of combustion gas forces acting on each rotor give rise to a pure torque: there exist no radial forces between the two rotors and the housing and no radial forces on the rotor bearings.
- (3) With the fan shaped working chambers and the linear variation of chamber shape, the HTRPE has the same advantage as the reciprocating engine, benefiting the flame spread and the combustion efficiency.
- (4) The period of the volumetric change in the HTRPE is 1/4 times that of the reciprocating engine and 1/6 times that of the Wankel engine, implying a higher power frequency.

As HTRPE has significant differences in its construction from existing engines, and many different components such as intake, exhaust, piston seals etc. are actively and consistently under development.

## References

- [1] R. STONE, Introduction to Internal Combustion Engines (3rd edn), MacMillian, New York, 1999.
- [2] S. Ashley, A new spin on the rotary engine, Mechanical Engineering, 117 (1995) 80-82.
- [3] D.-Y. LING, Z.-J. LIANG, X.-D. ZHU, A preliminary inquiry into the problems of the power transmission mechanism for internal combustion engine, Transactions of Chinese society of internal combustion engine, 8 (1985) 301-313.
- [4] H.G. Rosenkranz, CMC Scotch Yoke Engine Technology, in, Melbourne University, Victoria, 1998.
- [5] J. Karhula, Cardan gear mechanism versus slider-crank mechanism in pumps and engines, in, Lappeenranta University of Technology, Finland, 2008.
- [6] W. HE, Y.-T. WU, C.-F. MA, Research of air powered engine system using two-stage single screw expander, Chinese Journal of Mechanical Engineering (Chinese Edition), 46 (2010) 139-143.

- [7] R. Mikalsen, A.P. Roskilly, A review of free-piston engine history and applications, *Applied Thermal Engineering*, 27 (2009).
- [8] T. Korakianitis, M. Boruta, J. Jerovsek, P.L. Meitner, Performance of a single nutating disk engine in the 2 to 500 kW power range, *Applied Energy*, 86 (2009) 2213-2221.
- [9] I.S. Ertesvag, Analysis of the Vading concept-a new rotary-piston compressor, expander and engine principle, *Proceedings of the Institution of Mechanical Engineers, Part A: Journal of Power and Energy*, 216 (2002) 283-290.
- [10] K. Yamamoto, mazda rotary engine, Sankaido Co., Ltd, Tokyo, Japan, 1981.
- [11] B. Hudson, The Production of Power by Pure Rotary Means, in: architecture and design, RMIT University, Melbourne, Australia, 2008.
- [12] J. Roy J. Hartfield, Development of a Rotary Vane Gas Cycle Heat Engine, in: 44th AIAA/AIASAM-E20/S0A8-E4/7A0S3E E Joint Propulsion Conference & Exhibit, 2008.
- [13] R.G. Morgado, Internal combuston engine and method, in, 2007.
- [14] B. Librovich, R.W. Tucker, C. Wang, On gear modelling in multistage rotary vane engines, *Meccanica*, 39 (2004) 47-61.
- [15] J.O. Wieslaw, About a New Conception of Internal Combustion Engine Construction I. Rotary Engines, in: 2008 ASME International Mechanical Engineering Congress and Exposition, Boston, Massachusetts, USA.
- [16] M. CHENG, Y. ZHANG, J.-F. Zi, Differential velocity vane pump driven by rotating guide-bar-gear mechanism, *Chinese Journal of Mechanical Engineering (Chinese Edition)*, 42 (2006) 54-59.
- [17] L. LIANG, A rotary engine with two rotors and its design method, in, 2005.
- [18] H.F. CHUN, Alternative-step appliance rotary piston engine, in.
- [19] H. DENG, C.-Y. PAN, H.-J. XU, X. ZHANG, Theoretical research on the power transmission system of a twin-rotor piston engine, *Chinese Journal of Mechanical Engineering (Chinese Edition)*, 48 (2012) 64-68.
- [20] C.-Y. PAN, H. DENG, H.-J. XU, A piston engine with annular connecting cylinders, in, china, 2011.
- [21] C.-Y. PAN, H. DENG, H.-J. XU, Power transmission equipment composed of a pericycloidal mechanism and two double crank mechanisms, in, 2011.
- [22] H. DENG, C.-Y. PAN, X.-C. WANG, L. ZHANG, L. DENG, Comparison of two types of twin-rotor piston engine mechanisms, *J. Cent. South Univ. Technol.*, on print (2012).

### Biographical notes

Xiaojun Xu, born in 1972, is currently an associate professor in the College of Mechatronics Engineering and Automation, National University of Defense Technology, China. His research interests include power generating machine design, new energy resource utilization, intelligent machine and digital design. Tel: +86-731-84574931; E-mail: xuxiaojunmail@sina.com